A Research on the Effect of Velocity and Road Type on the Ride Smoothness of 16-Seat Passenger Buses Using a Mechanical Suspension System

Hung-Phi Cao
Vinh Long University of Technology Education, Vinh Long City, Vietnam
caohungphi@vlute.edu.vn

Thanh-Dong Nguyen
Vinh Long University of Technology Education, Vinh Long City, Vietnam
dongnt@vlute.edu.vn

Huu-Danh Tran
Vinh Long University of Technology Education, Vinh Long City, Vietnam
danhth@vlute.edu.vn (corresponding author)

Received: 2 August 2025 | Revised: 23 August 2025, 9 September 2025, and 28 September 2025 | Accepted: 5 October 2025

 DOI: https://doi.org/10.48084/etasr.13796

ABSTRACT

The vibration of cars and 16-seat passenger buses is affected by operating conditions such as velocity and road type. While in motion, the road surface creates vibrations that affect the vehicle and its passengers. Vibration acceleration, the maximum vertical acceleration of the vehicle body (a_{max}), is used to evaluate smoothness and the impact of vibration on passengers. To establish a basis for evaluating smoothness and determining the limit velocity on different types of roads, this article built and investigated a spatial dynamics model of 16-seat passenger buses with a mechanical suspension system. Based on the criteria selected for evaluating smoothness, the research results determined the corresponding limit velocity of smoothness levels for road types B, C, D, and E according to the ISO 8608:2016 standard, which ensures smoothness for passengers and drivers, especially during long trips. The results showed that a smooth feeling is achieved under operating conditions on type B roads with a velocity not exceeding 83.77 km/h, on type C roads with a velocity not exceeding 20.05 km/h, on type D roads with a velocity not exceeding 82.69 km/h, and on type E roads with a velocity not exceeding 19.82 km/h. The working limit is exceeded at a velocity greater than 89.64 km/h on type D roads and a velocity greater than 21.28 km/h on type E roads.

Keywords-16-seat passenger buses; smoothness; limit velocity; suspension

I. INTRODUCTION

The suspension system connects the vehicle body to the wheel axle, affecting the smoothness and safety of movement, especially on roads with poor surface quality, with each road imperfection transmitting, through the suspension system, to the vehicle and its occupants. Conversely, the static load of the vehicle and the dynamic load generated during oscillation will affect the road surface under the influence of the suspension system. A poor suspension system will cause dynamic forces to act on the road surface, damaging it, while the reaction force of the road on the wheel will affect the vehicle, reducing its smoothness and shortening the life of its parts, as well as causing wheel separation. Therefore, when studying the suspension system, it is necessary to analyze both the impact on the vehicle and its occupants and the interaction with the road [1]. A conventional suspension system includes an elastic element (e.g., a spring, leaf spring, pneumatic spring, or torsion bar), a damping element (e.g., a hydraulic damper), and guide elements [2, 3]. The suspension system is an important part of a vehicle, which reduces vibrations when the vehicle encounters disturbances from bumps in the road and smooths out the ride. At the same time, the car's vibrations generate dynamic loads that impact the road and cause damage to the road surface [1, 4]. Modern passenger buses often use suspension systems with elastic elements that can change stiffness, such as pneumatic elements. Poor control of stiffness can cause large oscillations and unstable vehicle bodies, which often cause discomfort for passengers and the driver [4]. Passenger buses are vehicles with high safety requirements that must ensure smoothness [5],

which is affected by structural factors of the suspension system, tire characteristics, vehicle structural factors, such as axle distance and vehicle center of gravity position, and operating conditions, such as velocity and road type [6]. There are many criteria for evaluating smoothness, involving: natural oscillation frequency, oscillation acceleration, smoothness coefficient, and critical amount of oscillation. The natural oscillation frequency depends only on structural parameters, while other criteria depend on both the structure and operating conditions, such as velocity and road type [7]. Currently, smoothness is a criterion specified in international standards, namely ISO 2631-1 [8] and BS 6841 [9]. To determine the limit velocity according to the standards, a seven-degree-of-freedom spatial model was built and examined with random pavement agitation according to the ISO 8608:2016 [10], using MATLAB/Simulink [11]. Authors in [12] optimized the suspension system of passenger cars using a multi-objective method with a vibration model and blocking method, analyzing the oscillations of the driver, car body, and wheels in response to the impact of the road surface and different modes of motion. The results provide optimal parameters for the suspension system, improving smoothness and traction, and enhancing comfort and safety. Additionally, research has analyzed the influence of road surface quality on dynamic loads and suspension systems in specific types of vehicles. Authors in [13] studied the impact of road surface quality on dynamic forces on the rear axle of a multipurpose forest firefighting vehicle, as well as the influence of suspension stiffness on vehicle frame loads [14]. Authors in [15] examined the effect of velocity and road quality on the dynamic load responses using a vehicle–bridge interaction model. However, these studies focused mainly on specialized vehicles and did not address the speed factor or evaluate smoothness according to international standards for passenger buses. The objective of this study is to examine how speed and road surface type influence the smoothness of 16-seat buses with mechanical suspension systems. The aim is to determine the appropriate speed limit for each type of road according to ISO 2631-1 and ISO 8608 standards.

II. METHODOLOGY

The paper's research method includes:

- Building a seven-degree-of-freedom spatial dynamics model for a 16-seat passenger car with a mechanical suspension system.
- Using the Newton-Euler equation to establish a system of differential equations that describe vertical motion.
- Simulating random road surface agitation according to the ISO 8608:2016 standard using the Simulink tool in Matlab.
- Examining the smoothness based on the maximum acceleration of the vehicle body (a_{max}) at speeds ranging from 10 km /h to 100 km/h on roads B, C, D, and E.
- Evaluating smoothness according to the ISO 2631-1 standard by dividing the corresponding speed limit zones.

III. CONTENT

A. Dynamic Model of 16-Seat Passenger Bus

Figure 1 shows the structure of the spatial dynamics model of a 16-seat passenger bus used to study smooth motion.

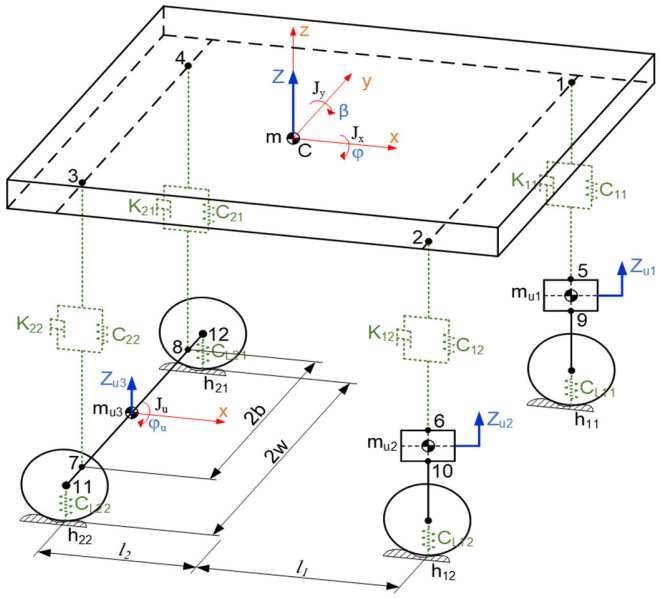

Fig. 1. Dynamic model of 16-seat passenger bus.

As shown in Figure 1, m is the sprung mass, while m_{u1}, m_{u2}, m_{u3} are the unsprung masses of the left front axle, right front axle, and rear axle, respectively. The displacement of the sprung mass in the z direction is Z, whereas Z_{u1}, Z_{u2}, Z_{u3} are the displacements of the unsprung masses of the left front axle, right front axle, and rear axle in the z direction. The moment of inertia of the sprung mass around the x axis and y axis are J_x and J_y, respectively, while the moment of inertia of the unsprung mass of the rear axle around the x axis is J_u. The rotation angle of the sprung mass around the x axis and y axis is φ, while the rotation angle of the unsprung mass of the rear axle around the x axis is φ_u. The stiffness of the elastic element of the suspension system is C_{ij} and the damping coefficient of the suspension system is K_{ij}. C_{Lij} is the stiffness of the elastic element of the tire radius, w is the distance from the vehicle center to the left/right wheel (m), b is the distance from the vehicle center to the left/right suspension connection point, l_1 and l_2 are the distances from the vehicle center to the front and rear axles, h_{ij} is the road surface bump height, 1, 2, 3, 4 are the connection points of the sprung mass to the suspension system, 5, 6, 7, 8 are the connection points of the unsprung mass to the suspension system, and 9, 10, 11, 12 are the connection points of the unsprung mass to the tire, with $i = 1$ for the front axle, $i = 2$ for the rear axles, $j = 1$ for the left side, and $j = 2$ for the right sides. To simplify the research process when constructing a vibration model of a 16-seat passenger bus, certain assumptions must be adopted. These assumptions reduce the complexity of modeling and calculations while maintaining the problem's generality and ensuring the required level of accuracy:

- The masses of the vehicle body and axles are symmetrically distributed with respect to the vertical plane running through the center of the vehicle.
- The vehicle is fully loaded with passengers, while the engine, drivetrain, passengers, and cargo are considered a rigid block that contributes to the body mass.
- The suspended and unsprung masses are considered absolutely rigid.
- The pitch and roll axes' positions remain constant relative to the vehicle's center of gravity during motion.
- The elastic characteristics of the suspension components, tires, etc., are assumed to be linear.
- The wheels are assumed to be in continuous contact with the road surface during motion. The road surface is considered non-deformable and the wheel–road contact is modeled as a point contact, while tire stiffness is considered constant and the damping effect of the tire is ignored.
- The influence of vibration excitation sources, such as the engine and drivetrain, is neglected and road irregularities are considered the sole source of excitation.
- The effects of wheel slip and aerodynamic drag on the vehicle are also neglected.

The model is based on the method of separating the multi-body system structure and using the Newton-Euler equation to create a system of differential equations that describes the car's vertical dynamics [5]. The model includes seven degrees of freedom: three degrees of freedom describe the motion of the sprung mass: Z, φ, and β, two degrees of freedom describe the motion of the unsprung mass of the front axle: Z_{u1} and Z_{u2}, and two degrees of freedom describe the motion of the unsprung mass of the rear axle: Z_{u3} and φ_u. The system of differential equations that describes the vertical dynamics of a 16-seat passenger bus for the sprung mass is illustrated in Figure 2:

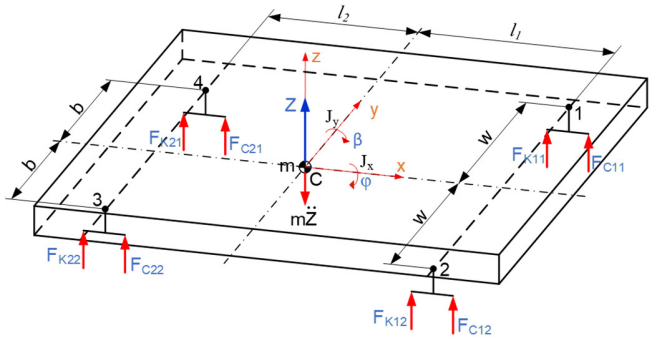

Fig. 2. Force model acting on the sprung mass.

$$m.\ddot{Z} = F_{K_{11}} + F_{K_{12}} + F_{K21} + F_{K22} + F_{C_{11}} + F_{C_{12}} + F_{C_{21}} + F_{C_{22}} \quad (1)$$

$$J_x.\ddot{\varphi} = (F_{K11} + F_{C11} - F_{K12} - F_{C12}).w + (F_{K21} + F_{C21} - F_{K22} - F_{C22}).b \quad (2)$$

$$J_y.\ddot{\beta} = -(F_{K11} + F_{C11} + F_{K12} + F_{C12}).l_1 + (F_{K21} + F_{C21} + F_{K22} + F_{C22}).l_2 \quad (3)$$

Figure 3 presents the force model for the unsprung mass of the front axle:

Fig. 3. Force model acting on the front axle (front view).

$$m_{u1}.\ddot{Z}_{u1} = -F_{K_{11}} - F_{C_{11}} + F_{CL11} \quad (4)$$

$$m_{u2}.\ddot{Z}_{u2} = -F_{K12} - F_{C12} + F_{CL12} \quad (5)$$

Figure 4 shows the force model of the unsprung of the rear axle:

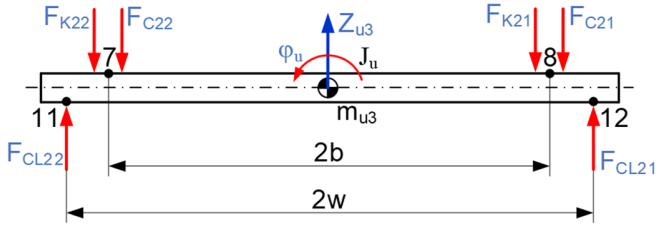

Fig. 4. Force model acting on the rear axle (front view).

$$m_{u3}.\ddot{Z}_{u3} = -F_{K21} - F_{C21} - F_{K22} - F_{C22} + F_{CL21} + F_{CL22} \quad (6)$$

$$J_u.\ddot{\varphi}_u = (-F_{K21} - F_{C21} + F_{K22} + F_{C22}).b + (F_{CL21} - F_{CL22}).w \quad (7)$$

where F_{Cij} is the elastic force of the suspension system (N), F_{Kij} is the suspension damping resistance force (N), and F_{CLij} is the radial elastic force of the tire (N). The internal forces of the suspension system, F_{Cij} and F_{Kij}, portrayed in Figure 5, cause the vehicle body to move vertically, as well as forward and backward and from side to side:

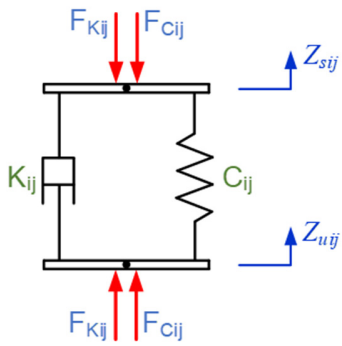

Fig. 5. Internal force model of the suspension system.

- Elastic force of the suspension system:

$$F_{Cij} = C_{ij}\left(Z_{u_{ij}} - Z_{sij}\right) \quad (8)$$

- Damping force of the suspension system:

$$F_{Kij} = K_{ij}\left(\dot{Z}_{uij} - \dot{Z}_{sij}\right) \quad (9)$$

- Radial elastic force of the tire:

$$F_{CLij} = C_{Lij}\left(h_{ij} - Z_{u_{ij}}\right) \quad (10)$$

where Z_{sij} is the displacement of sprung mass (m), and Z_{uij} is the displacement of unsprung mass (m).

- Points above the suspension system:

$$\begin{cases} Z_1 = Z + \varphi.w - \beta.l_1 \\ Z_2 = Z - \varphi.w - \beta.l_1 \\ Z_3 = Z - \varphi.b + \beta.l_2 \\ Z_4 = Z + \varphi.b + \beta.l_2 \end{cases} \quad (11)$$

- Points below the suspension system:

$$\begin{cases} Z_7 = Z_{u3} - \varphi_u.b \\ Z_8 = Z_{u3} + \varphi_u.b \\ Z_{11} = Z_{u3} - \varphi_u.w \\ Z_{12} = Z_{u3} + \varphi_u.w \end{cases} \quad (12)$$

Figures 6-8 provide an overview of the process for solving a system of differential equations, which describes the dynamics of a 16-seat passenger bus using MATLAB/Simulink. The diagram contains functional blocks, each representing a characteristic element of the model. Each functional block contains additional blocks that process input and output signals.

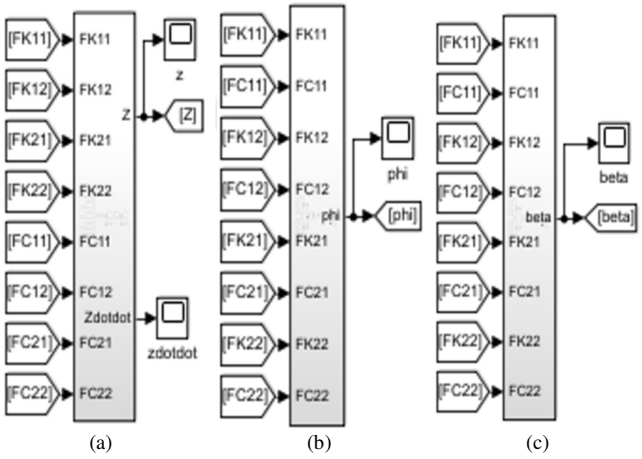

Fig. 6. Overall diagram of: (a) displacement of sprung mass in z direction, (b) rotation angle of sprung mass around x axis, and (c) rotation angle of sprung mass around y axis.

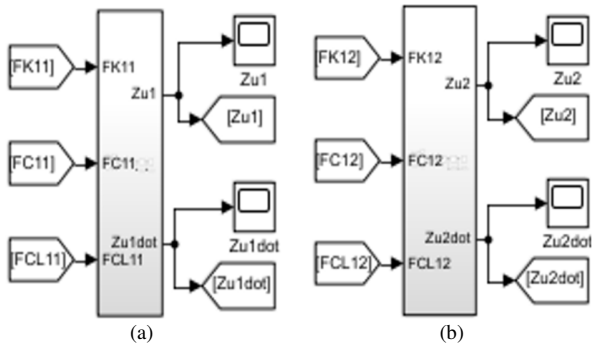

Fig. 7. Overall diagram of displacement of unsprung mass of: (a) left front axle, (b) right front axle in z direction.

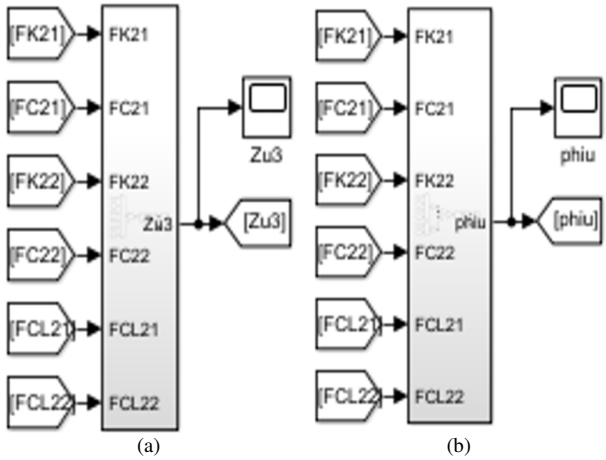

Fig. 8. Overall diagram of: (a) displacement of unsprung mass of rear axle in z direction, (b) rotation angle of unsprung mass of rear axle around x axis.

B. Excitation Function

The random agitation of the pavement is constructed according to ISO 8608:2016 [10] and is presented in Figure 9, which shows road types of decreasing surface quality, ranging from A to F. The height, $h(x)$, is determined by:

$$h(x) = \sum_{i=1}^{N} \sqrt{2.G_d(n_i).\Delta n}.cos(2\pi.i.\Delta n.x + \varphi_i) \quad (13)$$

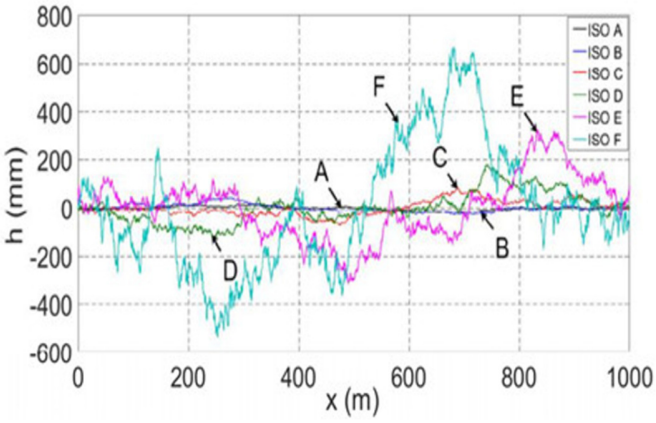

Fig. 9. Road surface irregular according to ISO 8608:2016.

C. Investigation Plans

This study examines road surface irregularities of types B, C, D, and E according to ISO 8608:2016. Sixteen-seat passenger buses move uniformly at velocities ranging from 10 km/h to 100 km/h (v10-v100) increasing by 5 km/h. To evaluate the smoothness of 16-seat passenger buses, the study used the technical and simulation parameters of the surveyed vehicle, a 16-seat Ford Transit passenger bus, as depicted in Table I. Some parameters that were not fully provided in the accompanying catalog for the Ford Transit were calculated and converted, while others were determined by collecting data directly from the vehicle.

D. Evaluation Criteria

A vehicle's smoothness depends on its structure, suspension system, tires, road surface, and driving technique. Criteria for evaluating smoothness include oscillation frequency, acceleration, mean square acceleration, and the smoothness coefficient [11]. The natural oscillation frequency depends only on the structural parameters of the oscillation system. The remaining criteria depend on operating conditions, such as velocity and road type. For the purposes of this study, the article selects maximum vertical acceleration of the vehicle body as the criterion for evaluating smoothness. According to the ISO 2631-1 standard, the smoothness levels used for evaluation are outlined in Table II [8].

TABLE I. TECHNICAL PARAMETERS OF 16-SEAT FORD TRANSIT PASSENGER BUS

Parameter	Value	Unit
Length × Width × Height	5998 × 2068 × 2775	mm
Wheelbase	3750	mm
Curb weight	2850	kg
Maximum permissible total weight	4100	kg
Front wheel track	1734	mm
Rear wheel track	1759	mm
Sprung mass (m)	3815	kg
Left front axle unsprung mass (m_{u1})	60	kg
Right front axle unsprung mass (m_{u2})	60	kg
Rear axle unsprung mass (m_{u3})	165	kg
Front axle suspension stiffness (C_{11}, C_{12})	27600	N/m
Rear axle suspension stiffness (C_{21}, C_{22})	40000	N/m
Front axle suspension damping coefficient (K_{11}, K_{12})	2295	Ns/m
Rear axle suspension damping coefficient (K_{21}, K_{22})	2550	Ns/m
Front axle tire stiffness (C_{L11}, C_{L12})	250000	N/m
Rear axle tire stiffness (C_{L21}, C_{L22})	300000	N/m

TABLE II. COMFORT LEVEL ASSESSMENT

a_{max} (m/s^2)	Ride comfort level
1,6	Very smooth
3,15	Smooth
6,3	Working limit

IV. RESULTS AND DISCUSSION

Figures 10-13 show the acceleration of the vehicle body at the center of gravity according to velocity on random road types (B-E). The survey results indicate that acceleration increases with speed and when road type changes from B to E [5, 11].

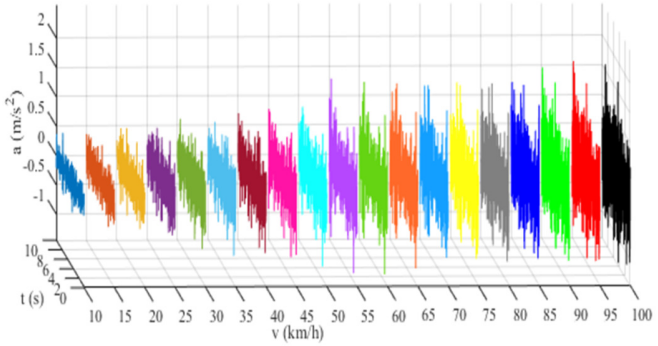

Fig. 10. Vehicle body acceleration on random road type B.

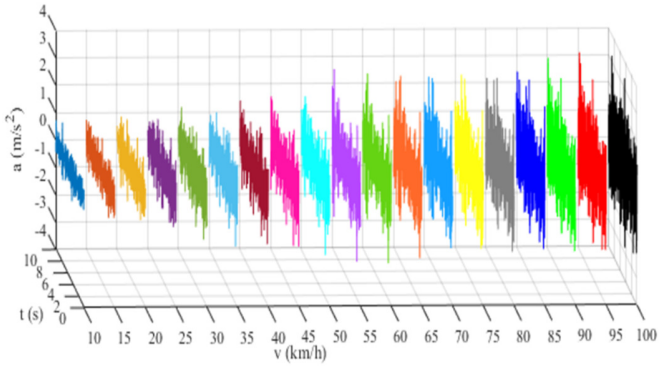

Fig. 11. Vehicle body acceleration on random road type C.

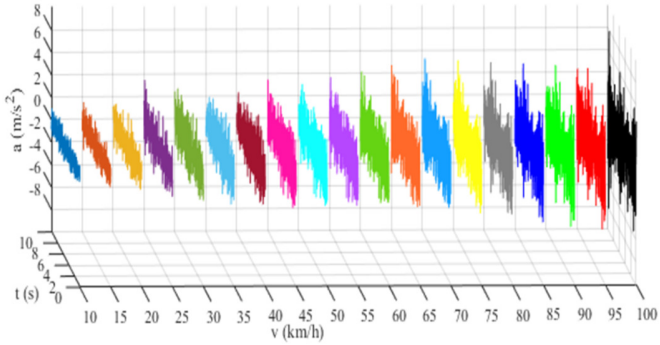

Fig. 12. Vehicle body acceleration on random road type D.

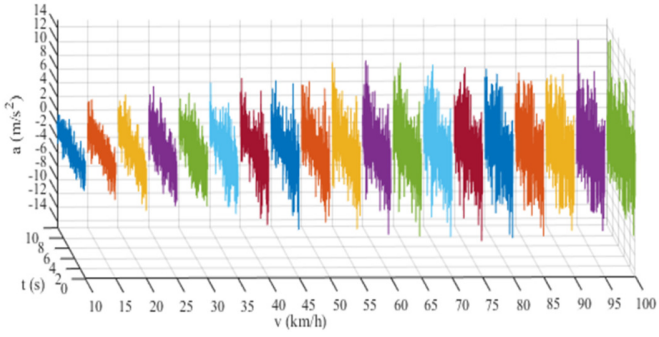

Fig. 13. Vehicle body acceleration on random road type E.

Figure 14 illustrates the maximum vertical acceleration (amax) of the vehicle body at the center of gravity according to

velocity on random road types B-E. The survey results show that a_{max} increases as velocity increases, when changing from road type B to E. Based on the limits in Table II, a_{max} can be divided into three zones: Zone I, "Very Smooth"; Zone II, "Smooth"; and Zone III, "Exceeds Working Limit." The vehicle's velocity limits on each road type are determined by the limit lines: $a_{max,gh}$ = 1.6 m/s², $a_{max,gh}$ = 3.15 m/s², and $a_{max,gh}$ = 6.3 m/s². Based on the above results, a very smooth feeling is achieved under operating conditions on type B roads with a velocity not exceeding 83.77 km/h, or on type C roads with a velocity not exceeding 20.05 km/h. A smooth feeling is achieved under operating conditions on type C roads with a velocity not exceeding 82.69 km/h, or on type D roads with a velocity not exceeding 19.82 km/h. The working limit is met under operating conditions on type D roads with a velocity not exceeding 89.64 km/h, or on type E roads with a velocity not exceeding 21.28 km/h. The working limit will be exceeded at a velocity greater than 89.64 km/h on type D roads, and at a velocity greater than 21.28 km/h on type E roads.

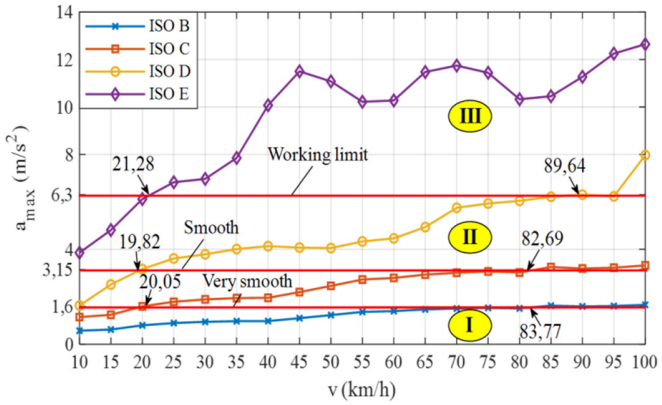

Fig. 14. Maximum acceleration (a_{max}) according to vehicle velocity.

TABLE III. MAXIMUM ACCELERATION VALUE (A_{MAX}) ACCORDING TO VELOCITY AND ROAD TYPE

Velocity v (km/h)	Road type			
	B	C	D	E
v10	0.5737	1.1474	1.6334	3.8583
v15	0.6208	1.2416	2.5203	4.8152
v20	0.7991	1.5982	3.1732	6.1187
v25	0.8958	1.7915	3.6167	6.8286
v30	0.9458	1.9477	3.7929	6.9707
v35	0.9738	1.9477	4.0130	7.8537
v40	0.9792	1.9583	4.1352	10.0728
v45	1.0999	2.1999	4.0757	11.5015
v50	1.2305	2.4611	4.0560	11.0790
v55	1.3647	2.7293	4.3348	10.2185
v60	1.3980	2.7959	4.4640	10.2762
v65	1.4685	2.9370	4.9386	11.4760
v70	1.5076	3.0152	5.7522	11.7458
v75	1.5352	3.0703	5.9335	11.4423
v80	1.5127	3.0253	6.0452	10.3253
v85	1.6284	3.2568	6.2194	10.4547
v90	1.5962	3.1924	6.3063	11.2716
v95	1.6136	3.2272	6.2345	12.2519
v100	1.6623	3.3246	7.9729	12.6465

Table III and Figure 15 present the maximum acceleration values (a_{max}) according to velocity from 10 km/h to 100 km/h on random road types ranging from B to E.

The determination of speed limit zones is based on the limits specified in Table II, and the smoothness criteria are presented in Figure 16. The maximum acceleration limit zone (a_{max}) is delineated by smoothness levels, which are defined as:

- Very smooth: the velocity of the system is constrained to a maximum of 1.6 m/s.
- Smooth: the maximum acceleration is between 1.6 m/s^2 and 3.15 m/s^2.
- Exceeding working limit: the operational limit is defined as an acceleration of 3.15 m/s^2 at the maximum, with a limit of 6.3 m/s^2.

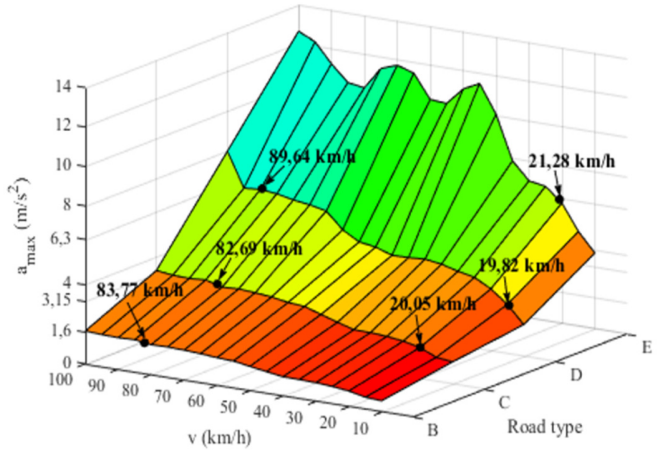

Fig. 15. Maximum acceleration value (a_{max}) according to velocity and road type.

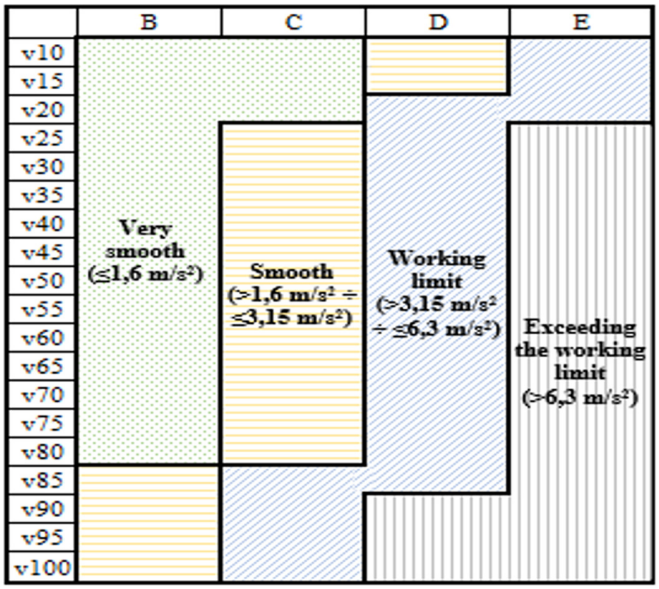

Fig. 16. Maximum acceleration limit zone (a_{max}) according to smoothness criteria.

The findings of this research indicate the feasibility of proposing adjustments to the velocity of 16-seat passenger buses, based on the type of road, to ensure a smooth driving experience. These recommendations can serve as a foundation for the development of regulations establishing velocity limits for different types of roads.

V. CONCLUSIONS

The road surface's deflection generates vibrations that are transmitted to the vehicle, affecting its durability, the well-being of its occupants, and the performance of its components. In the case of passenger buses, it is important to ensure the limit velocity according to the type of road to guarantee a smooth ride. The findings of the present research reveal that for 16-seat buses, the maximum permissible velocity for type B roads is 80 km/h, while for type C roads, it is 20 km/h, ensuring a very smooth driving experience. For type C roads, the maximum permissible velocity is 80 km/h, while for type D roads, it is 15 km/h, providing a smooth driving experience. To maintain the required level of smoothness, the maximum permissible velocity for type D roads is 85 km/h, whereas for type E roads, the maximum permissible velocity is 20 km/h. For type D roads, 16-seat passenger buses must not exceed 85 km/h, and for type E roads, they must not exceed 20 km/h, to ensure a smooth driving experience for passengers and drivers.

ACKNOWLEDGMENT

This work was supported by Vinh Long University of Technology Education (Vietnam).

REFERENCES

[1] D. Viet Ha, "Study on evaluating road-friendly suspension systems," *Journal of Science and Technology*, no. 4, pp. 112–115, Apr. 2021.

[2] S. Misaghi, C. Tirado, S. Nazarian, and C. Carrasco, "Impact of pavement roughness and suspension systems on vehicle dynamic loads on flexible pavements," *Transportation Engineering*, vol. 3, Mar. 2021, Art. no. 100045, https://doi.org/10.1016/j.treng.2021.100045.

[3] M. Yu, S. A. Evangelou, and D. Dini, "Advances in active suspension systems for road vehicles," *Engineering*, vol. 33, pp. 160–177, Feb. 2024, https://doi.org/10.1016/j.eng.2023.06.014.

[4] I. T. Jiregna and G. Sirata, "A review of the vehicle suspension system," *Journal of Mechanical and Energy Engineering*, vol. 4, no. 2, pp. 109–114, 2020, https://doi.org/10.30464/jmee.2020.4.2.109.

[5] T. M. Hung, "Optimal selection for an air suspension system on buses through a unique high level parameter in genetic algorithms," *Heliyon*, vol. 8, no. 3, Art. no. e09059, Mar. 2022, https://doi.org/10.1016/j.heliyon.2022.e09059.

[6] D. Viet Ha, "Study on the impact of speed and road type on the ride comfort of passenger cars equipped with air suspension systems," *Journal of Marine Science and Technology*, Special Issue, pp. 347–351, Oct. 2021.

[7] L. X. Long, L. V. Quynh, and B. V. Cuong, "Study on the influence of bus suspension parameters on ride comfort," *Vibroengineering Procedia*, vol. 21, pp. 77–82, Dec. 2018, https://doi.org/10.21595/vp.2018.20271.

[8] *ISO 2631-1:1997 Mechanical vibration and shock — Evaluation of human exposure to whole-body vibration*. Geneva Switzerland: International Standard Organization, 1997.

[9] *BS 6841:1987 Guide to measurement and evaluation of human exposure to whole-body mechanical vibration and repeated shock*. London, UK: BSI, 1987.

[10] *ISO 8608:2016 Mechanical vibration — Road surface profiles — Reporting of measured data*. Geneva, Switzerland: International Standard Organization, 2016.

[11] T. Xu, Z. Chen, Y. Liang, and L. Sun, "Evaluation of passenger comfort with road field test multi-axis vibration," *Journal of Vibroengineering*, vol. 23, no. 1, pp. 227–255, Dec. 2020, https://doi.org/10.21595/jve.2020.21578.

[12] T. T. An and N. V. Tuan, "Optimization of the Suspension System of Passenger Cars using the Vibration Model Multi-Objective Method," *Engineering, Technology & Applied Science Research*, vol. 14, no. 5, pp. 17019–17028, Oct. 2024, https://doi.org/10.48084/etasr.8260.

[13] V. V. Luong, H. P. Cao, T. T. Nguyen, and H. C. Ho, "Effect of road quality to dynamic load action on the rear axle housing multi-purpose forest fire fighting vehicle," *AIP Conference Proceedings*, vol. 2601, 2023, Art. no. 020028, https://doi.org/10.1063/5.0129522.

[14] A. Yavuz and S. E. Hacibektasoglu, "Evaluation of road roughness and vehicle speed effects on vibration comfort of school bus driver seats following the ISO 2631-1 standard and occupational health and safety legislation," *Bitlis Eren Üniversitesi Fen Bilimleri Dergisi*, vol. 12, no. 4, pp. 1171–1184, Dec. 2023, https://doi.org/10.17798/bitlisfen.1358965.

[15] B. Nunia, T. Rahman, S. Choudhury, and P. Janardhan, "Effect of vehicle speed and road surface roughness on the impact factor of simply supported bridges due to IRC Class A and B loading," *SN Applied Sciences*, vol. 2, 2020, Art. no. 923, https://doi.org/10.1007/s42452-020-2733-0.